

# Optical stirring in a droplet cell bioreactor

Murat Muradoglu,<sup>1</sup> Thuong Le,<sup>1</sup> Chun Yat Lau,<sup>1</sup> Oi Wah Liew,<sup>2</sup> and Tuck Wah Ng<sup>1,\*</sup>

<sup>1</sup>Laboratory for Optics, Acoustics, and Mechanics, Monash University, Clayton, VIC3800, Australia  
<sup>2</sup>Cardiovascular Research Institute, Centre for Translational Medicine, 14, Medical Drive, 117599 Singapore  
 \*engngtw@gmail.com

**Abstract:** In the context of a bioreactor, cells are sensitive to cues from other cells and mechanical stimuli from movement. The ability to provide the latter in a discrete fluidic system presents a significant challenge. From a prior finding that the location of the focus of a laser below particles relative to the beam axis producing a pushing effect in a predominant lateral sense, we advance an approach here that generates a gentle and tunable stirring effect. Computer simulation studies show that we are able to characterize this effect from the parameters that govern the optical forces and the movement of the particles. Experimental results with polystyrene microbeads and red blood cells confirm the notions from the simulations.

© 2012 Optical Society of America

**OCIS codes:** (170.4520) Optical confinement and manipulation; (170.3890) Medical optics instrumentation; (140.7010) Laser trapping.

## References and links

1. J. Chen, Z. Yu, L. Zhang, and G. Chen, "Microfluidic bioreactors for highly efficient proteolysis," *Curr. Chem. Biol.* **3**(3), 291–301 (2009).
2. H. N. Vu, Y. Li, M. Casali, D. Irimia, Z. Megeed, and M. L. Yarmush, "A microfluidic bioreactor for increased active retrovirus output," *Lab Chip* **8**(1), 75–80 (2008).
3. E. Figallo, C. Cannizzaro, S. Gerecht, J. A. Burdick, R. Langer, N. Elvassore, and G. Vunjak-Novakovic, "Micro-bioreactor array for controlling cellular microenvironments," *Lab Chip* **7**(6), 710–719 (2007).
4. M. He, J. S. Edgar, G. D. M. Jeffries, R. M. Lorenz, J. P. Shelby, and D. T. Chiu, "Selective encapsulation of single cells and subcellular organelles into picoliter- and femtoliter-volume droplets," *Anal. Chem.* **77**(6), 1539–1544 (2005).
5. S. Daniel, M. K. Chaudhury, and P. G. de Gennes, "Vibration-actuated drop motion on surfaces for batch microfluidic processes," *Langmuir* **21**(9), 4240–4248 (2005).
6. H. Y. Tan, T. W. Ng, A. Neild, and O. W. Liew, "Point spread function effect in image-based fluorescent microplate detection," *Anal. Biochem.* **397**(2), 256–258 (2010).
7. J. K. K. Lye, T. W. Ng, and W. Y. L. Ling, "Discrete microfluidics transfer across capillaries using liquid bridge stability," *J. Appl. Phys.* **110**(10), 104509 (2011).
8. J. J. Zhong, K. Fujiyama, T. Seki, and T. Yoshida, "A quantitative analysis of shear effects on cell suspension and cell culture of perilla frutescens in bioreactors," *Biotechnol. Bioeng.* **44**(5), 649–654 (1994).
9. W. Y. Sim, S. W. Park, S. H. Park, B. H. Min, S. R. Park, and S. S. Yang, "A pneumatic micro cell chip for the differentiation of human mesenchymal stem cells under mechanical stimulation," *Lab Chip* **7**(12), 1775–1782 (2007).
10. A. Ashkin, "History of optical trapping and manipulation of small-neutral particle, atoms, and molecules," *IEEE J. Sel. Top. Quantum Electron.* **6**(6), 841–856 (2000).
11. T. Iwaki, "Effect of internal flow on the photophoresis of a micron-sized liquid droplet," *Phys. Rev. E Stat. Nonlin. Soft Matter Phys.* **81**(6), 066315 (2010).
12. A. Vogel, V. Horneffer, K. Lorenz, N. Linz, G. Hüttmann, and A. Gebert, "Principles of laser microdissection and catapulting of histologic specimens and live cells," *Methods Cell Biol.* **82**, 153–205 (2007).
13. A. Siddiqi, T. W. Ng, and A. Neild, "Specific collection of adherent cells using laser release in a droplet-driven capillary cell," *J. Biomed. Opt.* **15**(6), 065003 (2010).
14. A. Ashkin, J. M. Dziedzic, J. E. Bjorkholm, and S. Chu, "Observation of a single-beam gradient force optical trap for dielectric particles," *Opt. Lett.* **11**(5), 288–290 (1986).
15. K. König, H. Liang, M. W. Berns, and B. J. Tromberg, "Cell damage in near-infrared multimode optical traps as a result of multiphoton absorption," *Opt. Lett.* **21**(14), 1090–1092 (1996).
16. U. Mirsaidov, W. Timp, K. Timp, M. Mir, P. Matsudaira, and G. Timp, "Optimal optical trap for bacterial viability," *Phys. Rev. E Stat. Nonlin. Soft Matter Phys.* **78**(2), 021910 (2008).
17. M. Muradoglu, W. S. Y. Chiu, and T. W. Ng, "Optical force lateral push-pulling using focus positioning," *J. Opt. Soc. Am. B* **29**(4), 874–880 (2012).

18. T. A. Nieminen, V. L. Y. Loke, A. B. Stilgoe, G. Knoner, A. M. Branczyk, N. R. Heckenberg, and H. Rubinsztein-Dunlop, "Optical tweezers computational toolbox," *J. Opt. A, Pure Appl. Opt.* **9**(8), S196–S203 (2007).
19. B. H. P. Cheong, V. Diep, T. W. Ng, and O. W. Liew, "Transparency-based microplates for fluorescence quantification," *Anal. Biochem.* **422**(1), 39–45 (2012).
20. H. Li, J. R. Friend, and L. Y. Yeo, "Microfluidic colloidal island formation and erasure induced by surface acoustic wave radiation," *Phys. Rev. Lett.* **101**(8), 084502 (2008).
21. J. Whitehill, A. Neild, T. W. Ng, and M. Stokes, "Collection of suspended particles in a drop using low frequency vibration," *Appl. Phys. Lett.* **96**(5), 053501 (2010).
22. H. Xia, J. Wang, Y. Tian, Q. D. Chen, X. B. Du, Y. L. Zhang, Y. He, and H. B. Sun, "Ferrofluids for fabrication of remotely controllable micro-nanomachines by two-photon polymerization," *Adv. Mater. (Deerfield Beach Fla.)* **22**(29), 3204–3207 (2010).
23. B. Weiss, W. Hilber, R. Holly, P. Gittler, B. Jakoby, and K. Hingerl, "Dielectrophoretic particle dynamics in alternative-current electro-osmotic micropumps," *Appl. Phys. Lett.* **92**(18), 184101 (2008).
24. J. A. King and W. M. Miller, "Bioreactor development for stem cell expansion and controlled differentiation," *Curr. Opin. Chem. Biol.* **11**(4), 394–398 (2007).
25. N. K. Inamdar, L. G. Griffith, and J. T. Borenstein, "Transport and shear in a microfluidic membrane bilayer device for cell culture," *Biomicrofluidics* **5**(2), 022213 (2011).
26. C. M. Potter, M. H. Lundberg, L. S. Harrington, C. M. Warboys, T. D. Warner, R. E. Berson, A. V. Moshkov, J. Gorelik, P. D. Weinberg, and J. A. Mitchell, "Role of shear stress in endothelial cell morphology and expression of cyclooxygenase isoforms," *Arterioscler. Thromb. Vasc. Biol.* **31**(2), 384–391 (2011).
27. K. Yamamoto, T. Sokabe, T. Watabe, K. Miyazono, J. K. Yamashita, S. Obi, N. Ohura, A. Matsushita, A. Kamiya, and J. Ando, "Fluid shear stress induces differentiation of Flk-1-positive embryonic stem cells into vascular endothelial cells in vitro," *Am. J. Physiol. Heart Circ. Physiol.* **288**(4), H1915–H1924 (2005).
28. J. R. Glossop and S. H. Cartmell, "Effect of fluid flow-induced shear stress on human mesenchymal stem cells: differential gene expression of IL1B and MAP3K8 in MAPK signaling," *Gene Expr. Patterns* **9**(5), 381–388 (2009).
29. Z. Yang, W. H. Xia, Y. Y. Zhang, S. Y. Xu, X. Liu, X. Y. Zhang, B. B. Yu, Y. X. Qiu, and J. Tao, "Shear stress-induced activation of Tie2-dependent signaling pathway enhances reendothelialization capacity of early endothelial progenitor cells," *J. Mol. Cell. Cardiol.* **52**(5), 1155–1163 (2012).
30. M. Morga-Ramírez, M. T. Collados-Larumbe, K. E. Johnson, M. J. Rivas-Arreola, L. M. Carrillo-Cocom, and M. M. Álvarez, "Hydrodynamic conditions induce changes in secretion level and glycosylation patterns of Von Willebrand factor (vWF) in endothelial cells," *J. Biosci. Bioeng.* **109**(4), 400–406 (2010).
31. Y. Ban, Y. Y. Wu, T. Yu, N. Geng, Y. Y. Wang, X. G. Liu, and P. Gong, "Response of osteoblasts to low fluid shear stress is time dependent," *Tissue Cell* **43**(5), 311–317 (2011).

## 1. Introduction

A bioreactor, in the context of cell culture, refers to a device or system meant to grow cells or tissues. Traditionally, cell cultivation processes required the screening of large numbers of cell lines in shake flask cultures. The need to carry out a vast number of development cultivations has led to the increasing widespread deployment of small-scale bioreactor systems that offer miniaturized and high throughput solutions. This has led to efforts in incorporating microfluidics [1–3] which has resulted in arguably the smallest bioreactor possible using optical tweezers [4]. In the realm of microfluidics, there is a trend towards the use of discrete volume systems that offer flexible and scalable system architectures as well as high fault tolerance capabilities [5–7]. Moreover, because sample volumes can be controlled independently, such systems have greater ability for reconfiguration whereby groups of unit parts in an array can be altered to change their functionality.

Cells are often sensitive to their microenvironment in which cues from other cells, and mechanical stimuli from movement are crucial [8,9]. The ability to provide the latter in a discrete fluidic system presents a significant challenge. The ability to use light to move matter is linked to the photophoresis effect. Direct photophoresis is caused by the transfer of photon momentum to a particle by refraction and reflection [10], when the particle is transparent and has an index of refraction larger compared to its surrounding medium. Indirect photophoresis occurs as a result of an increase in the kinetic energy of molecules when particles absorb incident light only on the irradiated side, thus creating a temperature gradient within the particle [11]. When the light beam is sufficiently focused, the forces developed are strong enough to detach cells from adherent surfaces in a technique known as laser catapulting [12,13]. Laser tweezing, alternatively, is accomplished through the gradient force component of a focused laser beam, which is strongest at the waist [14]. That this is also the location of highest intensity of the beam presents a problem in manipulating cells, where there have been

reports of photodamage [15,16]. Intuitively, the capacity to provide mechanical stimuli will benefit from a gentle ‘stirring’ of the contents within with as little photodamage as possible. Whilst it is conceivable that direct photophoresis may provide the means of doing this, such a system will generally be difficult to fabricate. An approach that locates the focus of the beam either above or below in order to pull and push particles relative to the beam axis in a predominant lateral sense was recently reported [17]. We show here that this approach offers the ability for generating a gentle and tunable stirring effect.

## 2. Approach

In region I in Fig. 1(a), the asymmetry of forces will result in the combined scattering and gradient forces pulling the particle laterally towards the beam axis and also upwards in the  $z$ -direction. In region II, the scattering and gradient forces work against each other resulting in a lateral force that pushes particles away from the beam axis. At some distance above the focal point these two forces come into equilibrium and trap the particle. At points beyond the equilibrium, the gradient force dominates by pulling particles downwards and laterally towards the beam axis creating an effective potential well.

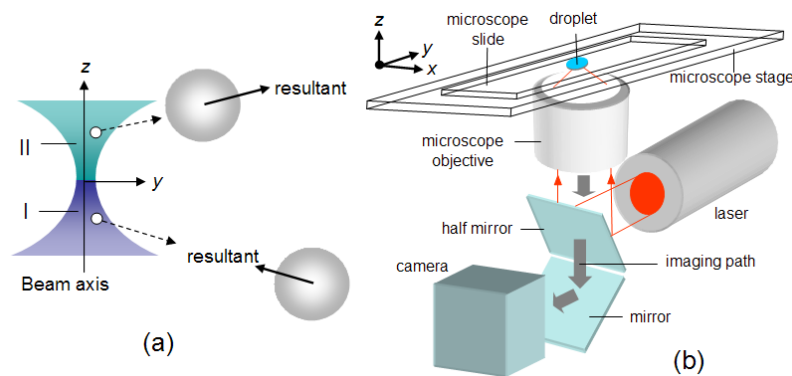


Fig. 1. (a) The geometry of an incident focused laser beam that gives rise to scattering and gradient forces such that the resultant forces when sphere located at regions below (I) and above (II) the focus moves the sphere towards and away from the beam axis respectively. The setup to accomplish optical stirring (b) involves focusing the laser beam close to the bottom surface of the droplet and using the microscope stage to move the slide and droplet in the  $x$ - $y$  plane.

In being able to stir effectively without the particle ever falling into the beam focus (where photodamage may occur) it would be necessary for the particle to only reside in the region denoted by II. We thus propose a system described in Fig. 1(b) whereby the laser beam is focused within the liquid medium but close to the bottom surface of the droplet. Coincidentally, this is also the region where the particles (if they are large enough) will settle by gravitational sedimentation. For sedimentation to be facilitated or hastened, an auxiliary light source from above can be used to create a photophoretic force downwards. Stirring is accomplished simply by moving the slide and droplet around in the  $x$ - $y$  plane using the microscope stage. One strategy will be to perform a line scan along the  $x$  direction followed by step movements in the  $y$  direction or vice-versa. The degree with which a particle ‘bounces off’ the laser beam center will depend on the relative position between the particle and beam center, the translator’s speed, the laser beam power for a specific particle’s refractive index and size, and hydrodynamic effects.

## 3. Numerical modeling

Spherical particles of sizes  $a \approx \lambda$ , where  $\lambda$  is the light wavelength, and  $a$  is the particle radius are known to violate the ray optics condition. In this regime we calculate the optical forces using the Generalized Mie-Lorentz Theory (GMLT) [18]. We simulate with an incident  $x$ -

polarized TEM<sub>00</sub> Gaussian beam under a numerical aperture (NA) of 0.98 and wavelength of 1.06 $\mu\text{m}$ . The surrounding medium is assumed to be water with a refractive index of  $n = 1.33$ . Placing polystyrene particles with a refractive index of 1.59 and 3 $\mu\text{m}$  radius at a grid of points we produced and stored a map of the optical force efficiency. The units of optical force efficiency  $Q$ , can be related to the optical force,  $F$ , by  $F = nPQ/c$  in which  $P$  is the beam power at the focus, and  $c$  is the speed of light in free space. In carrying out the optical force simulation, we found that we had to significantly limit the grid size due to the rapidly growing number of expansion terms required at points far from the focal point. Due to the inherent rotational symmetry about the z-axis, we limit our calculations to only the x-z plane. Once a map of  $Q$  over the x-z plane in region II was obtained, the dynamic equations of motion were applied to an inertial frame, i.e. the microscope stage moving at a constant speed,  $v_p$ , over the fixed laser beam. In this model, the very low Reynolds number (much less than 1), dictates that the Stokes drag term is linearly dependent on velocity. Hydrodynamic effects associated with the relative position of the particle to the coverslip walls were neglected.

#### 4. Experimental

Experimentation was done on a conventional laser single beam trapping system (Cell Robotics Inc.) operating at a wavelength of 1064nm and having a rated full power of 5W. Video sequences were captured using a video camera (Moticam 2000) and digitized for image analysis. Polystyrene beads of 6 $\mu\text{m}$  diameter (Bangs Laboratories) were used. In order to reduce sticking to surfaces, Triton-X100 reagent (Sigma Aldrich) was added to the bead suspension. The bead solution was then placed as droplet in a circular shallow chamber created by varnish or silicone tape [19]. The laser trap was operated using a 60X objective having a numerical aperture (NA) of 0.98. Similar experiments were also conducted with red blood cells from sheep (R3378 Sigma Aldrich). These samples, originally in dry powder form and glutaraldehyde treated, were rehydrated using 0.9% sodium chloride solution.

#### 5. Results and discussion

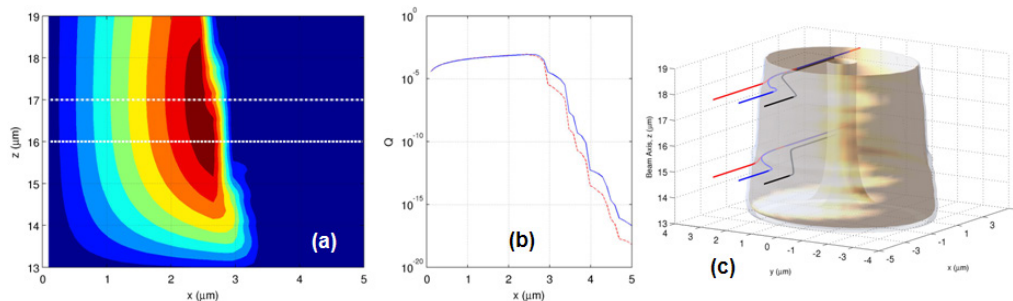


Fig. 2. (a) Contour plot of the optical force efficiency,  $Q$ , in the x-z plane beyond the transition line. (b) Plot of optical force efficiency,  $Q$ , along  $z = 16\mu\text{m}$  and  $z = 17\mu\text{m}$  as indicated by the solid and dashed lines, respectively. The optical force efficiency drops off rapidly after 3.5 $\mu\text{m}$ . Based on this observation we safely neglect optical force calculations beyond 8 $\mu\text{m}$  to lessen computational demands. The trajectories of particles at different starting locations with  $z = 15\mu\text{m}$  and  $z = 18\mu\text{m}$  is shown in (c). The magnitude of the sum of x and y force components is rendered in as an iso-surface. The line colors indicate the entry point of particles in the x-y plane, with black being at  $x = 4\mu\text{m}$ ,  $y = 0.5\mu\text{m}$ , blue at  $x = 4\mu\text{m}$ ,  $y = 1.5\mu\text{m}$ , and red at  $x = 4\mu\text{m}$ ,  $y = 2.5\mu\text{m}$ .

We begin with the beam modeling results. The calculated optical force efficiency,  $Q$ , in the x-z plane is shown in Fig. 2. As previously reported, the transition from pulling to pushing occurs at some distance above the focal point of the laser beam [17], which in this case is at 13 $\mu\text{m}$ . As can be seen in Fig. 2(a), the optical force efficiency is highest at around  $z = 16.5\mu\text{m}$  at a lateral distance of about 2.5 $\mu\text{m}$  away. Beyond a lateral distance of 3 $\mu\text{m}$ , the order of  $Q$  drops rapidly as is shown in Fig. 2(b). This limits the region of influence of the laser. Based on this observation, we safely approximate the optical force at points beyond 8 $\mu\text{m}$  as zero.

The trajectory of a particle at various starting positions with respect to the laser beam is shown in Fig. 2(c), where the shaded iso-surface represents the magnitude of the summed optical force. One finds the deflection effect less pronounced when the particle is further away from the path passing through the beam center. Also the deflection is not strictly planar, although it will appear to be when viewed through the microscope. Nevertheless, the significant lateral deflection should give rise to a stirring effect.

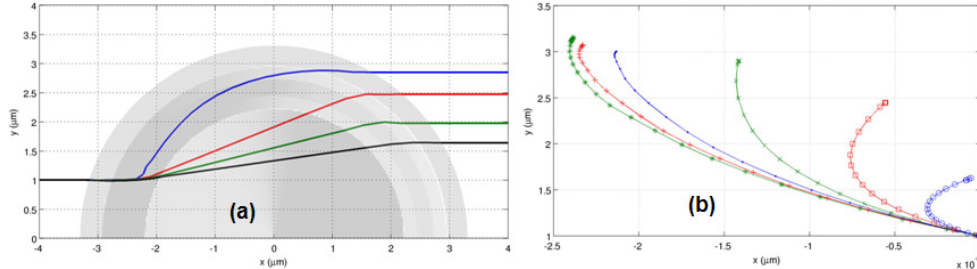


Fig. 3. (a) Plot of particle trajectories at optical powers 10mW (black), 15mW (green), 20mW (red), 35mW (blue) at  $z = 19\mu\text{m}$ . (b) Plot of local displacements of particles on microscope stage for  $z = 16\mu\text{m}$  at various power levels starting from the right to left, 10mW (blue-circle), 20mW (red-box), 25mW (green-cross), 40mW (blue-dotted), 100mW (red-star) and 200mW (green-star). The optical stirring effect can be controlled by changing laser power.

The displacement of the particle at various laser powers with respect to the stationary laser and moving stage are shown in Figs. 3(a) and 3(b), respectively. The results show that the extent of stirring of the particles can be controlled by varying the applied power. The stirring effect saturates at higher laser powers since the order of the optical force efficiency drops rapidly after  $3\mu\text{m}$ , as was shown in Fig. 2(b).

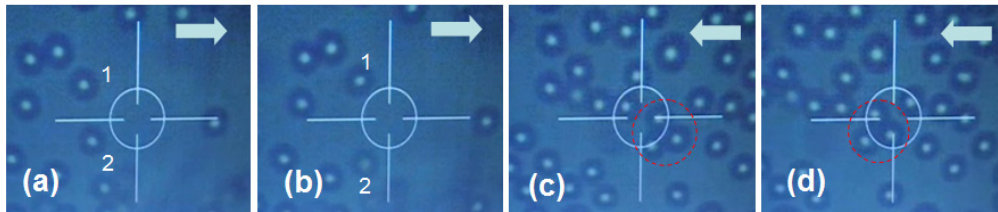


Fig. 4. With the laser beam located axially below the polystyrene beads and having sufficient power, the image sequence (a) before and (b) after shows the particles numbered 1 and 2 laterally pushed away from the beam center. With the laser beam located axially below the polystyrene beads but having insufficient power, the image sequence (c) before and (d) after shows the cluster of particles circled in red unaffected by the beam. The arrow shows the general direction of travel of the particles(see Media 1).

The experimental results shown in Figs. 4-5 comply with the modeling results. With 40% power, the polystyrene particles identified as 1 and 2 in Figs. 4(a)–4(b) can be seen to depart from their general motion paths such that they are pushed away from the laser beam center. The manner of the pushing is more strongly lateral rather than axial, which confirms a gentle stirring effect. That the particles never meet the beam center also meant that the propensity for photothermal or phototoxicity damage is diminished. When the laser beam power was reduced to 10%, one finds the cluster of particles identified in Figs. 4(c)–4(d) being able to move past the laser beam center almost without being affected. Hence, the optical stirring effect requires a certain threshold for operation. This is consistent with the modeling results.

The optical stirring effect was found to be operational with red blood cells as well, as indicated in Fig. 5 This illustrates the viability of the method applied to living organisms. A modeling of the forces will be more involved due to the shape complexity of these cells over simple shapes such as spheres and rods. The experimental results, however, indicate that a simple scaling effect, as far as the optical stirring effect is concerned, may be in operation.



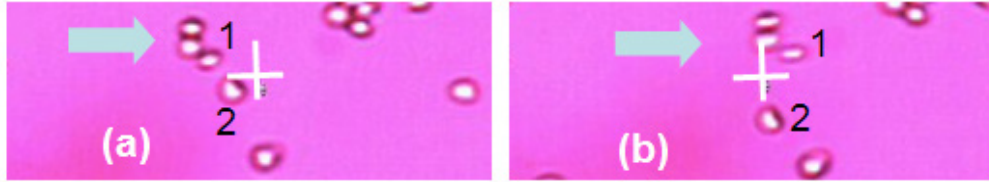


Fig. 5. With the laser beam located axially below the particles and having sufficient power, the image sequence (a) before and (b) after shows the red blood cells numbered 1 and 2 laterally pushed away by the beam. The arrow shows the general direction of travel of the cells (see Media 1).

At this juncture, we should mention that acoustic [20,21], magnetic [22], and dielectrophoretic [23] devices are also able to create a swirling motion that is able to move particles and cells around. The strong motion of material within the liquid medium associated with the effect will generally not be amenable for cells or to guide cells towards desired differentiation or biological response pathways. In both bioreactor and micro-bioreactor scale culture, a delicate balance or trade-off has to be reached in terms of the need to provide a perfusion or mixing function and controlling hydrodynamic shear stress. While perfusion and mixing provides a more homogenous environment by maintaining dissolved oxygen and nutrient concentrations and serves to reduce media cytotoxicity via recirculation effects, the consequent hydrodynamic shear forces, if on a high magnitude, are generally considered to have an adverse impact on cell survival and proliferation [24]. This is especially the case for shear sensitive cell types [25]. Evidences from studies also show that shear stress can have a significant influence on cellular morphology, growth patterns, and biological responses [26,27]. Different magnitudes of hydrodynamic shear stress evoke differential gene expression in signaling pathways in human bone marrow derived mesenchymal stem cells [28] and human endothelial progenitor cells [29], induce important changes in secretion and assembly of glycoproteins in mammalian cell cultures [30] as well as influence proliferation and osteoblastic differentiation [31]. Hence, in the setting of a static discrete droplet format, the gentle stirring afforded by our optical approach provides advantages of preserving cellular integrity and viability apart from promoting fidelity of biochemical and differentiation responses during cell culture and/or when performing cell-based assays.

## 6. Conclusions

The location of the focus of a laser below particles relative to the beam axis is known to produce a predominant pushing effect in the lateral sense. By moving the medium containing particles past a laser beam arranged in this manner, we have been able to develop an approach that creates a gentle and tunable stirring effect of particles. The computer simulations performed, enabled us to trace the expected deflection trajectories of the particles. Since the deflection effect is not enhanced beyond a certain laser power, this can be used as basis to find optimal powers for stirring. Experiments using polystyrene micro-beads and red blood cells confirm the optical stirring effect. This approach portends the capability to execute mechanical stimuli of cells in a small liquid volume bioreactor that is free of flow, leading to better realization of photonic lab-on-a-chip systems.

## Acknowledgments

This work is made possible by funding from the Australian Research Council DP120100583. TW is thankful for the insight and inputs provided by Michael Berns at the Beckman Institute, UCI.